Progress in Natural Science: Materials International 36 (2026) 31–41

HOSTED BY

Contents lists available at ScienceDirect

Progress in Natural Science: Materials International

journal homepage: www.elsevier.com/locate/pnsmi

# Noble metal-based electrocatalysts for acidic water electrolysis: Design strategies, AI-empowered approaches, and industrialization prospects

Xuan Yang[a,b], Chenfei Xu[b,c], Ziqi Fu[a,b], Xiaoyang Wang[a,b,*], Yanan Chen[a,b,**]

[a] State Key Laboratory of Precious Metal Functional Materials Tianjin University Tianjin, 300350, PR China
[b] School of Materials Science and Engineering, Key Laboratory of Advanced Ceramics Machining Technology of Ministry of Education, Tianjin Key Laboratory of Composite and Functional Materials, Tianjin University, Tianjin, 300072, PR China
[c] Joint School of National University of Singapore and Tianjin University, International Campus of Tianjin University, Fuzhou, 350207, PR China

ARTICLE INFO

*Keywords:*
Oxygen evolution reaction (OER)
Proton exchange membrane water electrolysis (PEMWE)
Artificial intelligence (AI)
Machine learning (ML)
High-throughput screening (HTS)

ABSTRACT

Proton exchange membrane water electrolysis (PEMWE) has long been regarded as a promising technology for hydrogen production due to its high electrolytic efficiency, reliability, and rapid response to renewable energy sources. Currently, noble metals and their oxides—such as Pt, $IrO_2$, and $RuO_2$—remain the most widely used and high active electrocatalysts in acidic media to accelerate the water electrolysis processes. However, their large-scale pratical application is severely hindered by the factors such as scarcity and the trade-off between activity and stability. Recently, the integration of artificial intelligence (AI) with high-throughput synthesis technology has demonstrated an increasingly vital role in material screening, enabling the design of highly efficient and cost-effective catalysts. This paper first reviews the fundamental catalytic mechanisms of the hydrogen evolution reaction (HER) and the oxygen evolution reaction (OER) in acidic media. Then, it summarizes the design strategies and prevailing challenges for noble metal catalysts in acidic water electrolysis. Finally, it presents several data-driven, synergistic approaches enabled by AI in noble metal catalyst research and development (R&D), along with the latest progress, current challenges, and future prospects.

## 1. Introduction

### 1.1. Development background and strategic value of PEMWE

Proton exchange membrane water electrolysis (PEMWE) represents a pivotal pathway for large-scale green hydrogen production. Its strategic significance is underscored by two distinct advantages [1–3]: (i) Efficiency and Compatibility: PEMWE operates at high current densities ($\geq$1 A $cm^{-2}$) with rapid dynamic response rates, making it highly compatible with the intermittent nature of renewable energy sources like solar and wind, thus supporting carbon neutrality goals. (ii) High-Purity Output: Compared to alkaline electrolysis, PEMWE delivers hydrogen with purity exceeding 99.999 %, facilitating its direct utilization in sensitive downstream applications such as fuel cells [4]. However, technical bottlenecks persist. While the cathodic hydrogen evolution reaction (HER, $2H^+ + 2e^- \rightarrow H_2$) is efficiently catalyzed by mature Pt-based materials (often achieving overpotentials <50 mV) [5], the anodic oxygen evolution reaction (OER, $2H_2O \rightarrow O_2 + 4H^+ + 4e^-$) remains the primary obstacle [6]. The OER involves a complex four-electron transfer process characterized by a high energy barrier and sluggish kinetics, rendering it the rate-determining step for the overall electrolysis efficiency. Furthermore, the highly corrosive acidic environment (e.g., 0.5 M $H_2SO_4$),imposes stringent stability requirements on the electrocatalysts. Consequently, the widespread industrialization of PEMWE is currently constrained by the urgent need for high-performance, cost-effective OER electrocatalysts [7–9].

Noble metal-based catalysts, especially iridium (Ir) and ruthenium (Ru), remain the most prevalent choices for acidic OER. Among them, Ir-based catalysts are the only commercial catalysts capable of long-term stability in acidic OER, though their intrinsic activity requires improvement [10–12]; Ru-based catalysts exhibit higher activity but are prone to overoxidation into soluble $RuO_4^{-1}$. Commercial PEMWE systems typically feature noble metal loadings of 2–3 mg $cm^{-2}$, resulting in high-cost drawbacks. Meanwhile, current non-noble metal catalysts such as oxides of cobalt or manganese are prone to dissolution in acidic environments [13–15], and thus cannot yet fully replace noble metals.

* Corresponding author. State Key Laboratory of Precious Metal Functional Materials Tianjin University Tianjin 300350, PR China.
** Corresponding author. State Key Laboratory of Precious Metal Functional Materials Tianjin University Tianjin, 300350, PR China.
*E-mail addresses:* xywang53@tju.edu.cn (X. Wang), yananchen@tju.edu.cn (Y. Chen).

https://doi.org/10.1016/j.pnsc.2025.12.007
Received 25 November 2025; Received in revised form 11 December 2025; Accepted 16 December 2025
Available online 30 December 2025

Current research on noble metal catalysts focuses on addressing the following core issues: Firstly, the trade-off between activity and stability [16]: The primary research emphasis lies in suppressing the dissolution of noble metals (e.g., Ir overoxidation and Ru leaching) while enhancing their intrinsic activity [11,12]. Secondly, high performance under low noble metal loading: designing effective non-noble metal supports that synergize with noble metal catalysts to reduce noble metal loading and preserve catalytic activity under high potential and oxidative condition [10]. Additionally, deepening studies of material design and catalytic mechanism through in situ characterization techniques (e.g., X-ray absorption spectroscopy (XAS) and transmission electron microscopy (TEM)) and density functional theory (DFT) calculations to reveal active site mechanisms aids in understanding catalyst mechanisms and designing next-generation catalysts [17,18]. Finally, leveraging artificial intelligence (AI) combined with high-throughput synthesis technologies empowers catalyst material screening and performance-structure relationships understanding [19].

## 2. The electrochemical basis and the role of noble metal catalysts

### 2.1. Reaction mechanisms and kinetic barriers

Acidic HER is one of the core reactions of PEMWE (Fig. 2a) (see Fig. 1). The acidic environment imposes extremely high demands on the chemical stability and corrosion resistance of catalysts. Platinum (Pt)-based materials remain the most effective HER catalysts currently available [20]. Nevertheless, other types of catalysts with outstanding performance also exist, such as single-atom catalysts: CuRh single-atom alloys exhibit an HER overpotential of only 34 mV@10 mA $cm^{-2}$ in 0.5 M $H_2SO_4$, along with a Tafel slope of 18.8 mV $dec^{-1}$, outperforming commercial Pt/C (37 mV) and maintaining stability for over 100 h [21]. This enhanced performance is attributed to Cu-O-Rh bridging oxygen groups stabilizing the single-atom structure and facilitating electron transfer. Additionally, metal–organic framework (MOF) -based catalysts such as the $NiRu_{0.13}$-BDC catalyst exhibit an extremely low overpotentials (13 mV at 10 mA $cm^{-2}$) in 1 M HCl solution, significantly lower than the typical value (approximately 30 mV) for commercial Pt/C catalysts [22]. Similarly, the Ru/Co-N-C-800 °C catalyst achieves a 13 mV overpotential at 10 mA $cm^{-2}$ in 0.5 M $H_2SO_4$ and exhibits faster reaction kinetics (Tafel slope of 23.3 mV $dec^{-1}$) [23]. These outstanding performances are attributed to the high surface area, tunable pore structure, and optimized electronic properties of the MOF framework, along with the high dispersion and efficient utilization of active atoms, which enhance hydrogen adsorption free energy and accelerate reaction kinetics. In summary, these materials exhibit Pt-like activity and outstanding stability in acidic HER by optimizing electronic structures and exposing more active sites. Benefiting from abundant $H^+$ provided by the acidic environment, HER requires only a two-electron transfer. Their catalyst designs—such as single-atom alloys and amorphous structures—facilitate optimization of hydrogen adsorption energy, enabling low overpotentials and high stability with fewer limiting factors.

In contrast, the anodic OER is constrained by high energy barriers, catalyst corrosion, and complex restructuring, making it the rate-determining step for overall water splitting [24]. The OER process involves two common mechanisms: the Adsorption Evolution Mechanism (AEM) and the Lattice Oxygen Mechanism (LOM) [25] (Fig. 2b and c). In AEM, the four-electron transfer process involves multiple proton-electron coupling steps, where the formation or desorption of *OOH typically acts as the rate-determining step (RDS), leading to a high theoretical overpotential [26]. In acidic OER electrocatalysis, the LOM involves direct the participation of lattice oxygen atoms in O-O bond formation. This generates $O_2$ through coupling of oxygen species at adjacent metal sites, thereby circumventing the linear scaling limitations inherent in the AEM and enhancing reaction kinetics [27,28]. However, while imparting high activity, the persistent involvement of lattice oxygen triggers surface reconstruction, oxygen vacancy ($O_V$) accumulation, and metal peroxidation. This accelerates catalyst dissolution and phase transitions, leading to structural instability in the LOM mechanism. This effect intensifies Ir or Ru ion leaching at elevated potentials [29], limiting long-term durability. Consequently, future breakthroughs in water electrolysis technology must prioritize developing acid-stable OER catalysts (e.g., via bridging oxygen groups or heterostructures) to balance the kinetic disparity between HER and OER [30–33]. This also represents the design direction for high-performance electrolyzers.

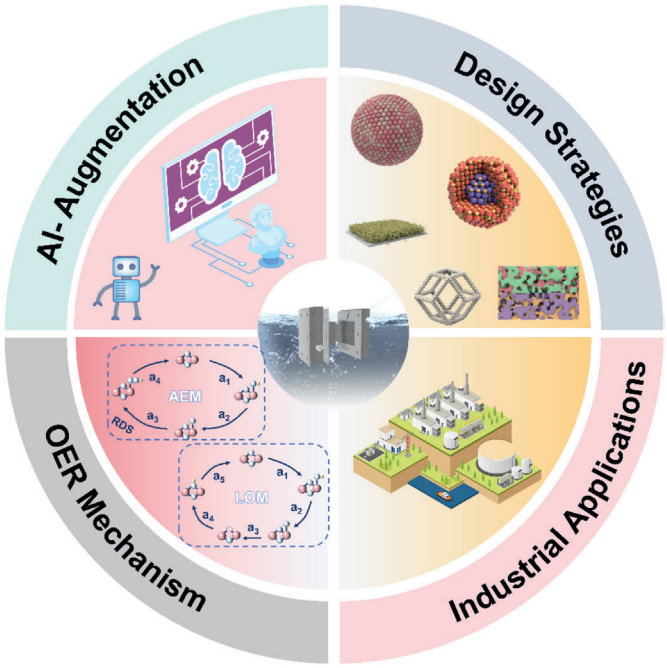


**Fig. 1.** Noble metal - based electrocatalysts for acidic water electrolysis: Design strategies, AI acceleration, mechanistic insights, and industrialization.

### 2.2. Key properties of noble metal catalysts

Noble metals (such as Ru and Ir) possess partially filled d orbitals, which endow their electronic structures with high tunability and enable optimization of adsorption energies with reaction intermediates, rendering them highly active sites [34]. First, their d-band centers typically lie close to the Fermi level—for example, the d-band center of Ru ranges from −1.13 eV to −1.39 eV—which enhances the interaction strength between the metal and adsorbed species such as *OOH or *O [35]. Shifting the d-band center upward, for instance through lithium (Li) intercalation or doping, increases the adsorption energy for oxygen intermediates, thereby lowering the reaction energy barrier. Second, the presence of coordinatively unsaturated sites (CUS) on noble metal oxides (e.g., $RuO_2$) provides highly active centers (such as $Ru^{4+}$ sites) that facilitate four-electron transfer processes. For example, Ru sites exposed on the (110) crystal plane of $RuO_2$ efficiently adsorb $OH^-$ and convert it to $O_2$ [36,37]. Upon doping with Mn or Li, the increased electron density at these sites further optimizes the formation energy of *OOH. Moreover, the bonding between noble metals and oxygen exhibits moderate covalency (Ru-O bond covalency can be weakened by doping), balancing reactivity and stability. Tin (Sn) or barium (Ba) doping elongates the Ru-O bond length from 1.97 Å to 2.00 Å, thereby reducing Ru-O covalency [38,39]. This diminishes lattice oxygen involvement (LOM pathway) and shifts toward a more efficient AEM pathway, thereby enhancing the intrinsic activity.

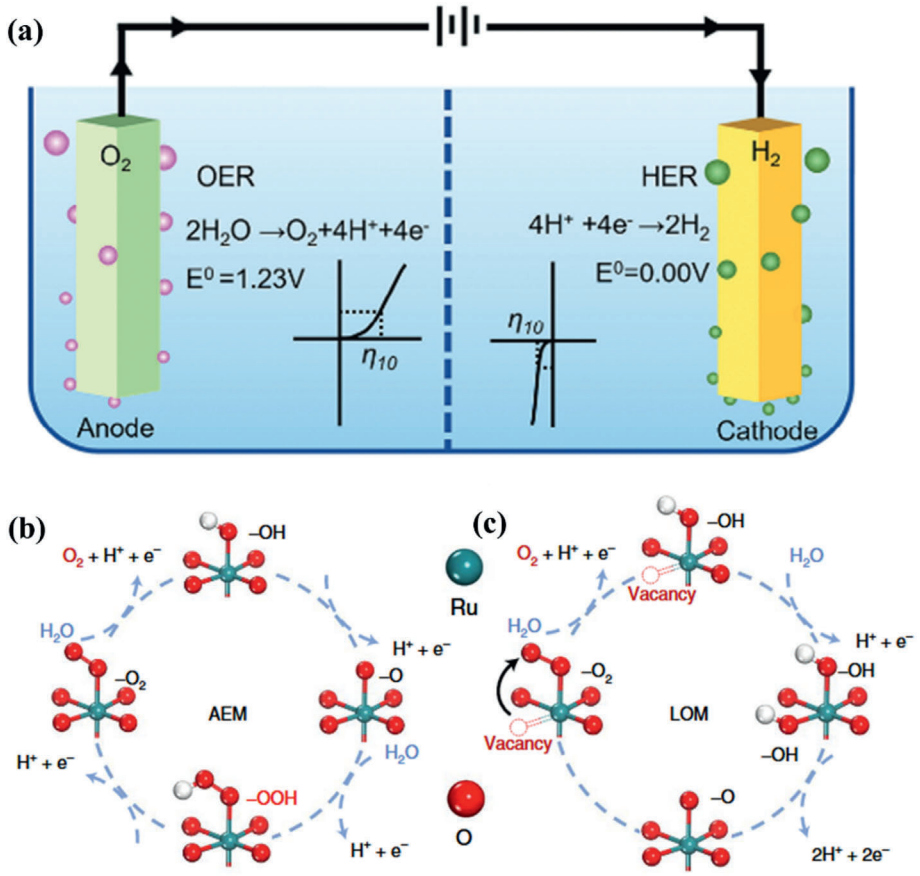


**Fig. 2.** (a) Electrochemical water splitting in acidic condition [34]. Copyright 2024, Wiley-VCH. Schematic of the simplified OER mechanism of ruthenium-based electrocatalysts for (b) AEM. (c) LOM [28]. Copyright 2021, Springer Nature.

Noble metal catalysts exhibit superior stability in acidic OER. Common stabilization strategies include: First, noble metal oxides (such as $IrO_2$ and $RuO_2$) form thermodynamically stable passivation layers in acidic environments, which resist dissolution and demonstrate high corrosion resistance. An integrated Ir-Ru anode was fabricated via passivation engineering, comprising a Ti substrate [40], a perovskite ($MnTiO_3$) passivation layer, and an Ir-Ru oxide catalytic layer (Fig. 3a–d), achieving stable operation exceeding 3000 h. Second, the d-orbital electrons of noble metals effectively regulate valence states, leveraging electronic structural stability to prevent excessive oxidation. $Ru^{4+}$ remains stable during OER, whereas non-noble metals (e.g., Mn or Co) readily oxidize to high valence states (e.g., from $Mn^{4+}$ to $Mn^{7+}$), causing structural collapse. Li or Ba doping reduces Ru oxidation states (e.g., from +4.0 to +3.96) via electron donation, suppressing over-oxidation of Ru and thereby minimizing $O_V$ formation and metal dissolution [35,39]. Finally, most noble metal oxides possess robust crystal structures that tolerate lattice oxygen loss. Doping (e.g., with Ba or Sn) introduces tensile strain [38], strengthening Ru-O bonds, inhibiting $O_V$ migration, and enhancing crystal structural stability (Fig. 3e–f).

In summary, noble metal catalysts, particularly Ir- and Ru-based materials, play an irreplaceable role in the electrocatalytic oxygen evolution reaction. This is primarily attributed to their unique electronic structural properties—including the coordination ability of unsaturated d orbitals and stability at high oxidation states. Building upon this deep understanding of the intrinsic properties of noble metal catalysts, AI methods can integrate discrete electronic structure parameters into a quantitative framework for stability prediction [41], thereby establishing a new paradigm for rational catalyst design (Fig. 3g). This approach holds promise for simultaneously enhancing the performance of noble metal catalysts while effectively reducing their loading.

## 3. AI-enabled catalyst development

### 3.1. AI for screening and prediction

In acidic electrocatalytic reactions (OER and HER), the development of noble metal catalysts (e.g., Ru-, Ir-, and Pt-based materials) faces challenges including high costs, low stability, and complex reaction mechanisms. AI and machine learning (ML), leveraging data-driven paradigms, have remarkably expedited high-throughput catalyst screening, accurate performance prediction, and rational catalyst design in electrocatalysis research.

Literature mining accelerates catalyst screening: leveraging an AI-assisted framework combining large language models (LLMs) and genetic algorithms (GAs) for high-entropy alloy (HEA) catalyst selection (Fig. 4a). The LLM extracted key active elements (e.g., Fe, Co, Ni, Pt) from 14,242 HER-related papers [42], thereby reducing candidate elements from 90 to 10 and consequently narrowing the Pt-based HEA combinations from 43.9 million to 126. GA then iteratively optimized (only 4 rounds with 24 samples) to select the optimal catalyst (e.g., IrCuNiPdPt/C), achieving a HER overpotential as low as 25.5 mV at 10 mA $cm^{-2}$, representing a 60 % efficiency improvement over traditional brute-force searches. This approach achieved “hour-scale” discovery through high-temperature thermal shock synthesis and electrochemical testing, highlighting AI's advantage in reducing experimental iterations.

Model training and performance prediction: ML models predict key catalytic metrics (e.g., overpotential, adsorption energy, stability) by training on material structure and property data from large databases such as materials project and open quantum materials database (OQMD) [44]. In Ru-based catalyst design, a back-propagation neural network

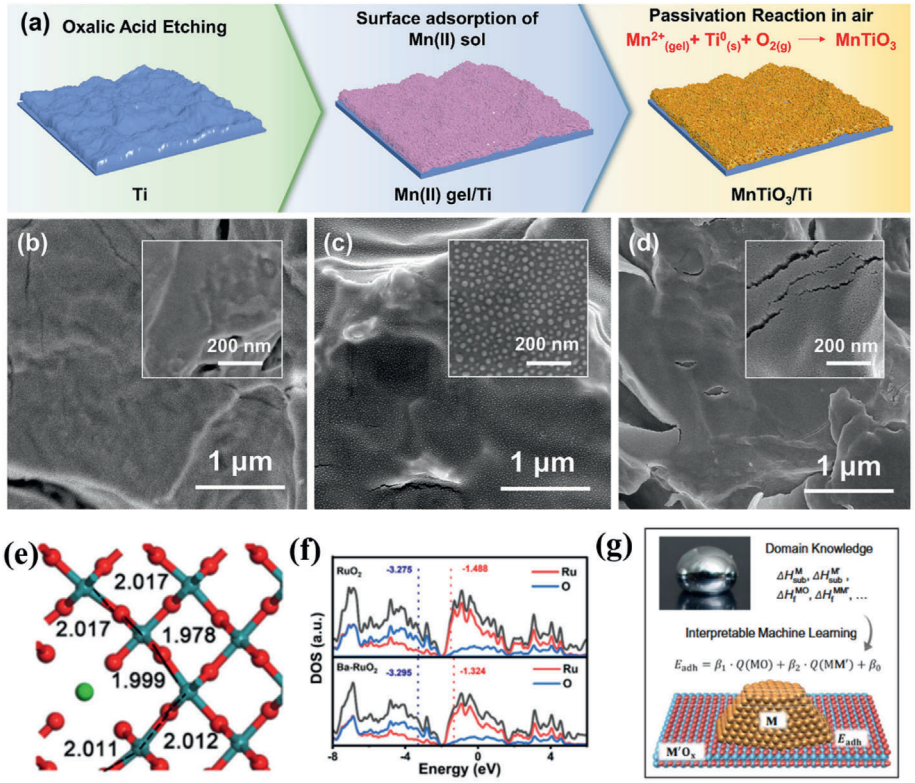


**Fig. 3.** (a) Schematic diagram of the preparation of the $MnTiO_3$ transition layer. Scanning electron microscopy (SEM) images of the electrode surface, (b) etched Ti substrate, (c) Mn(II) Gel-coated substrate, (d) $MnTiO_3$ transition layer [40]. Copyright 2025, American Chemical Society. (e) Structure models of Ba–$RuO_2$. (f) Calculated density of states (DOS) curves for $RuO_2$ (110) and Ba–$RuO_2$ (110) [39]. Copyright 2025, Elsevier. (g) A derivable formula was identified through interpretable ML [41]. Copyright 2024, AAAS.

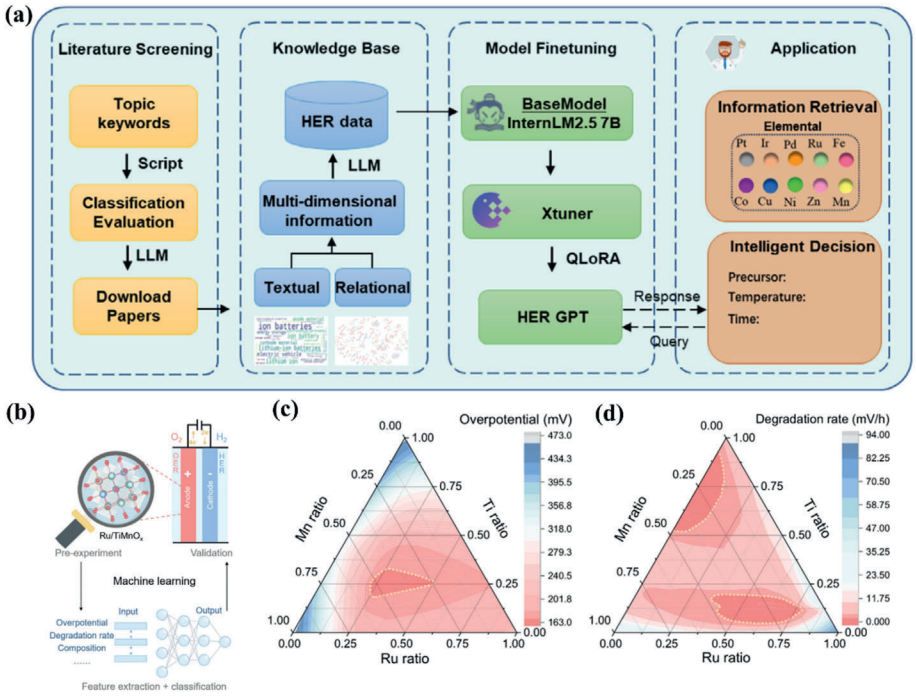


**Fig. 4.** (a) Framework overview of LLM, consisting of four main phases: literature screening, knowledge base construction, model fine-tuning, and application [42]. Copyright 2025, Wiley-VCH. (b) Overall ML diagram, showing the steps of experimentation, feature extraction, and validation. (c) Predicted OER overpotential and (d) deactivation rate with various ternary compositions [43]. Copyright 2025, Springer Nature.

was employed to screen Ru-Ti-Mn ternary compositions [43], predicting OER overpotential and deactivation rate (Fig. 4b–d). Bayesian optimization algorithms can be employed to optimize synthesis parameters for $Ru/TiMnO_X$ electrodes. The model identified an optimal composition range (Ru: 0.20–0.50, Ti: 0.20–0.30, Mn: 0.25–0.50), predicting overpotentials as low as 163.0 mV. Experimental validation confirmed the

$Ru_{0.24}/Ti_{0.28}Mn_{0.48}O$ (165.2 mV) electrode demonstrated high-quality activity, exhibiting approximately 49 × , 113 × , and 75 × higher activity than $RuO_2$ under acidic, neutral, and alkaline conditions, respectively, along with outstanding long-term durability exceeding 3000 h. This study demonstrates an AI-guided vapor deposition strategy that efficiently covers a vast design space with only 735 experiments, achieving significant efficiency gains.

### 3.2. Data-driven rational design

By integrating multi-source data, cross-scale simulations, and automated experiments, AI enables synergistic advancement in the development of noble metal catalysts—from atomic-level mechanism understanding to macroscopic performance prediction. This approach helps elucidate catalytic mechanisms and guides material optimization.

In catalyst design, multiscale modeling correlates catalyst performance across multiple dimensions—from electronic structure and atomic arrangement to phase stability and surface reconstruction. While traditional DFT calculations provide accurate energy descriptions, their computational cost limits large-scale screening. The integration of machine learning interatomic potential (MLIP) with active learning enables efficient simulation of atomic-scale behavior in multicomponent alloys. For instance, Maulana et al. employed an MLIP coupled with replication-exchange molecular dynamics (REMD/MC) (Fig. 5a–c) to investigate the atomic-scale mixing and surface segregation behavior of $Ru_X(Ir, Fe, Co, Ni)_{1-X}$ multicomponent alloys [45]. This approach successfully predicted the formation of primary face-centered cubic (FCC) and secondary hexagonal close-packed (HCP) phases, consistent with experimental observations, and provided a mechanistic explanation for Ru stability in multicomponent alloys. Furthermore, Abed et al. developed an AI-based high-throughput screening framework grounded in Pourbaix stability. By training a graph convolutional neural network (CGCNN-HD) model [46], they screened over 36,000 mixed metal oxides to predict their electrochemical stability (Fig. 5d–e). This work highlights the critical role of AI combined with multiscale modeling in reducing DFT computational costs and enabling high-throughput stability prediction.

Big data-driven catalyst design relies on an efficient closed-loop between high-throughput computational screening and experimental validation. Active learning significantly reduces the number of experiments by employing an iterative "predict-experiment-update" strategy, focusing on the most promising candidate materials. The CRESt platform (Copilot for Real-world Experimental Scientists) proposed by Zhang et al. serves as a benchmark in this field [47]. This system integrates LLMs, vision-language models (VLMs), and robotic automation to explore over 900 catalyst compositions and perform 3500 electrochemical tests within three months (Fig. 5f). It ultimately discovered an octahedral catalyst Pd-Pt-Cu-Au-Ir-Ce-Nb-Cr with a 9.3-fold improvement in cost-specific performance [47]. Furthermore, another breakthrough in AI lies in multimodal data fusion, integrating multi-source information including composition, structure, images, and text to construct more comprehensive catalyst characterization. Within the CRESt platform, the system analyzes microstructural features via SEM images, diagnoses experimental anomalies using VLM, and proposes corrective measures, achieving high reproducibility and automation throughout the experimental process.

However, when conducting AI simulations, high-dimensional material spaces with sparse data inevitably arise. Uncertainty quantification (UQ) and progressive learning strategies are crucial for avoiding overfitting and enhancing extrapolation capabilities. Nair et al. employed an ensemble SISSO approach, constructing a model collection via bootstrap sampling and monte carlo dropout (MC Dropout) to quantify prediction uncertainty (Fig. 5g) and define a Probability of feasibility (POF) to guide sample selection [48]. This work screened 12 acid-stable electrocatalysts from 1470 oxides in just 30 active learning iterations, significantly improving screening efficiency and reliability. Xu et al. developed an active learning framework based on an incremental learning strategy [49], combining DFT with sure independence screening and sparsifying operator (SISSO) to screen nine high-performance catalysts from 261 single-atom-doped metal oxides. Among these, MnSA-$RuO_2$ and FeSA-$TiO_2$ exhibited theoretical overpotentials below 0.3 V. This work demonstrates the advantages of AI in identifying descriptors and optimizing target performance.

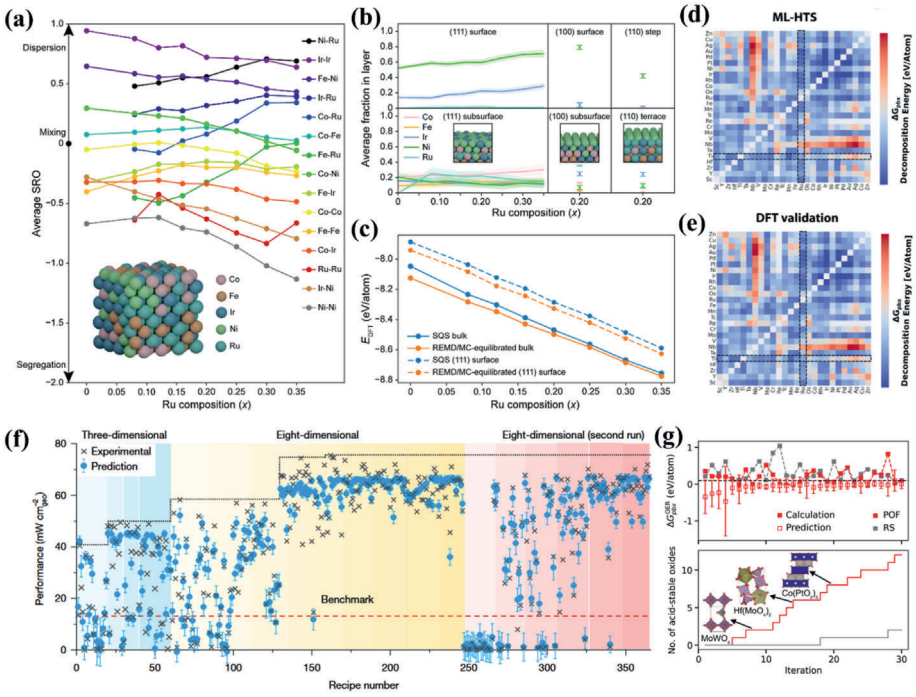


**Fig. 5.** (a) Bulk short-range order (SRO) analysis indicating atomic pairing and mixing behavior. (b) Surface and subsurface elemental distribution revealing segregation trends across different crystal facets. (c) Energy validation comparing DFT-calculated energies of relaxed configurations, confirming simulation reliability [45]. Copyright 2025, American Chemical Society. (d) ML and (e) DFT stability heatmap comparison: Ru-Ti identified as optimal [46]. Copyright 2024, American Chemical Society. (f) The complete AL campaign plot with the baseline AL model, with the performance value compared with the recipe number [47]. Copyright 2025, Springer Nature. (g) Superiority of probability of feasibility over random selection in active learning for acid-stable oxide discovery [48]. Copyright 2025, Springer Nature.

### 3.3. Potential challenges of AI in catalyst design

Beyond mere performance prediction, AI and ML are evolving to enable closed-loop catalyst development, particularly when synergized with automation technologies [50]. For instance, interpretability tools like SHAP (SHapley Additive exPlanations) can identify critical descriptors—such as metal-oxygen bond formation enthalpy and ionic radius—to rationally guide dopant selection. In parallel, active learning frameworks employing Bayesian optimization and generative models (e.g., MatterGen) significantly accelerate the exploration of vast chemical spaces by reducing the computational burden of DFT calculations. Furthermore, the integration of automated synthesis platforms (e.g., AI-EDISON) is realizing end-to-end autonomy, spanning from initial design to final characterization.

Despite these achievements, AI-driven catalyst design faces distinct challenges. (i) Model Generalizability: Current models are often trained on specific systems, highlighting an urgent need for universal descriptors applicable across diverse material classes. (ii) Data Quality: The heavy reliance on high-fidelity DFT and experimental datasets necessitates the establishment of standardized databases and multimodal data fusion. (iii) Dynamic Modeling: Capturing transient behaviors, such as surface reconstruction and dissolution under reaction conditions, remains a formidable task. Looking ahead, future research should focus on developing autonomous "AI chemists" via reinforcement learning, integrating real-time in situ characterization, and leveraging generative models to discover novel catalyst architectures.

In summary, AI leverages multi-scale modeling, high-throughput screening, and other technologies to establish a closed-loop optimization system for noble metal catalyst R&D, encompassing "data-model-experiment." Key future trends include: (1) Cross-scale dynamic simulation (integrating AI with operando characterization to analyze real-time structural evolution during catalytic operation); (2) Generative AI (designing novel catalyst compositions and microstructures); (3) Federated learning and data sharing (integrating multi-source data while protecting intellectual property to enhance catalyst databases); (4) Autonomous robotic experimentation (achieving full automation across "computational design - synthesis - characterization - testing"). These advancements propel catalyst development into a new era of rational design driven by big data and empowered by AI. As AI technology evolves, ML will enable closed-loop "design-synthesis-testing" cycles across more catalytic systems, ushering the field into an intelligent new age.

## 4. Catalyst design and engineering challenges

### 4.1. Ir-based catalysts: from single-component to structural engineering

The scarcity and prohibitive cost of iridium severely constrain the economic feasibility of gigawatt-scale PEMWE deployment. With $IrO_2$ priced at $4269.05 per troy ounce (2025), the high anodic Ir loading (1–2 mg $cm^{-2}$)—far surpassing cathodic Pt loading—remains a critical system cost driver [51,52]. Moreover, traditional Ir-based catalysts are limited by poor active site dispersion and low utilization efficiency, often requiring loadings exceeding 3.5 wt% [51]. This structural limitation is highlighted by the disparity in ECSA: close-packed Ir catalysts achieve only 34.8 mF/$cm^2$ compared to 71.4 mF/$cm^2$ for honeycomb structures, underscoring the poor site exposure in conventional designs [53]. To address these challenges, research strategies have evolved from single-component optimization tuning to multiscale structural engineering, targeting improved intrinsic activity and stability while maximizing iridium utilization [54].

Early design strategies focused on controlling the crystallinity, particle size, and phase of pure $IrO_2$ to expose more active sites. For instance, comparisons between crystalline and amorphous $IrO_2$ indicated that the amorphous phase exhibits higher initial activity but poorer stability [55]. Theoretical calculations indicate that the OER on pure $IrO_2$ follows AEM, but is constrained by the high energy barrier of the *OOH intermediate [56], resulting in a high overpotential (>300 mV). Design efforts at this stage primarily involved adjusting sintering temperatures and morphology control (e.g., nanoparticles), requiring large amounts of Ir with limited efficiency. Subsequently, introducing $O_V$ [57], metal vacancies, or foreign atom doping has been employed to modulate electronic structure and intermediate adsorption energies [58]. IrNiO generates Ir vacancies through electrochemical Ni leaching, forming d-band holes that shorten the Ir-O bond to 1.91 Å. This enhances *OOH adsorption, boosting mass activity by 90-fold compared to $IrO_2$ [59]. $H_2/N_2$ plasma treatment of $TiO_2$ nanowires generates O vacancies [60], which, combined with Sr single-atom adsorption, strengthens Ir-substrate interactions and reduces overpotentials for OER (250 mV)/HER (32 mV). The core of defect engineering lies in breaking scaling relationships, but requires balancing defect density to avoid structural degradation. Additionally, constructing core-shell, supported, or epitaxial heterojunctions enhances conductivity and stability through interfacial synergy [61]. Epitaxial growth of $IrO_2$ on homogeneous $SnO_2$ (with lattice mismatch <5 %) forms a tight interface. Epitaxial strain optimizes oxygen adsorption [62], achieving an OER mass activity of 503 mS $cm^{-1}$. Partial Ir single-atom embedding into NiO surfaces triggers Co-Ti synergistic centers via Ir-Ni second-shell interactions (increasing coordination number to 8) [63], following the LOM with a low overpotential of 263 mV and high stability over 350 h $CeO_2/IrO_2$ 3D/2D heterojunctions reduce OER activation energy through charge redistribution [64], achieving >900 mA $cm^{-2}$ current density in PEMWE. Such designs enable atomic-level interface control but involve high synthesis complexity. Recently, AI-assisted design of Ir-based catalysts has emerged as a cutting-edge strategy to address the scarcity of noble metal and enhance catalytic performance. By integrating Bayesian optimization, interpretable descriptors, and enhanced atomic structure representations, these methods efficiently explore complex material spaces, enabling atomically precise control. For example, in the Ir-$TiO_2$ system, Bayesian learning combined with DFT accelerated the identification of optimal surface compositions and $O_V$, guiding the synthesis of atomically dispersed Ir catalysts. These catalysts demonstrated a 23-fold increase in mass activity along with a 115 mV reduction in overpotential compared to commercial $IrO_2$ [65].Furthermore, interpretable AI models such as the ARSC descriptor (atomic properties (A), reactants (R), synergistic effects (S), and coordination effects (C)) unify activity prediction across diverse electrocatalytic reactions (e.g., OER, ORR) by decoupling atomic properties, reactants, synergistic effects, and coordination effects [66]. This approach guided the design of dual-site catalysts (e.g., Co-Ir systems) that demonstrated outstanding bifunctional oxygen catalytic activity in experiments. For complex interfacial structures, equivariante graph neural networks enhance atomic structure representations through message passing, overcoming chemical motif similarity challenges. They achieve high accuracy with descriptor prediction errors below 0.09 eV on disordered surfaces (e.g., HEAs) and supported nanoparticle systems, providing a reliable computational foundation for multi-level structural engineering [67–69]. These AI strategies not only reduce traditional trial-and-error costs but also deepen understanding of electronic structure regulation mechanisms through physically interpretable models. Synergizing with atomic-scale synthesis and in situ characterization, they propel iridium-based catalysts toward efficient, low-energy commercial applications.

In summary, the design of Ir-based catalysts has evolved from single-component optimization to multi-level structural engineering. The core trend involves regulating electronic structures through the synergistic effects of nanostructures, defects, and heterojunctions to optimize OER pathways (e.g., transitioning from AEM to LOM/OPM). Future efforts should focus on atomically precise synthesis, in-situ characterization, and AI-assisted design to address Ir scarcity and achieve commercialization.

### 4.2. Ru-based catalysts: the activity-stability trade-off

Ru-based catalysts have long dominated the performance landscape of acidic OER catalysts due to their moderate oxygen intermediate adsorption energy (the linear relationship between $\Delta G_{*OOH}$ and $\Delta G_{*O}$ approaches the peak of the volcano plot) [70]. In early studies, Ru-based catalysts served as benchmark materials. While exhibiting promising initial activity, they faced an inherent stability limitation that hindered industrial applicability [71]. However, recent structural design innovations have driven significant performance breakthroughs: First, nanostructuring: Recently reported Er-$RuO_X$ catalysts regulate Ru-O covalency via lanthanide elements (Fig. 6a), forming porous lamellar nanostructures with a specific surface area of 64.78 $m^2\ g^{-1}$ [72]. In PEMWE, they achieve 3 A $cm^{-2}$ at just 1.837 V with 35.5-fold enhanced stability. Subsequently, the single-atom dispersion strategy significantly enhances atomic utilization. By anchoring Ru single atoms at the atomic level onto $Co_3O_4$ nanorod carriers [73], outstanding performance was achieved in acidic OER (0.5 M $H_2SO_4$): with a low overpotential of 138 mV (10 mA $cm^{-2}$), mass activity as high as 1966 A $g^{-1}_{Ru}$, and stable operation exceeding 120 h at 100 mA $cm^{-2}$. DFT calculations and XAS analysis indicate that Ru single-atom dispersion shifts the d-band center from −1.72 eV to −1.58 eV, optimizing the adsorption energy of *OOH intermediates (ΔG reduced by 0.5 eV). Concurrently, charge redistribution weakens the Ru-O covalent bond (Ru-O bond length increased from 1.50 Å to 1.53 Å). *OOH intermediate (ΔG reduced by 0.5 eV). Concurrently, charge redistribution weakened the Ru-O covalent bond (Ru-O bond length increased from 1.50 Å to 1.53 Å) (Fig. 6b), effectively suppressing Ru peroxidation and dissolution while promoting a stable AEM. A currently prevalent alloy/heterojunction design strategy further modulates the electronic structure via a synergistic Co-doped Ru@$RuO_2$ core-shell heterojunction architecture (Fig. 6c) [10], thereby affording a low overpotential of 203 mV at 10 mA $cm^{-2}$ and a high mass activity of 108.4 A $g^{-1}_{Ru}$ for the OER in acidic electrolyte. Notably, this catalyst exhibits excellent long-term stability with continuous operation exceeding 400 h at 10 mA $cm^{-2}$. DFT calculations demonstrated a downward shift of the d-band center (from −1.20 eV to −1.32 eV) for Ru active sites, along with a stress-induced attenuation of Ru-O covalent interactions—evidenced by a decrease in the Integrated Crystal Orbital Hamiltonian Population (ICOHP) value from 2.76 eV to 2.65 eV. These electronic and structural modulations collectively lowered the free energy barrier of the rate-determining step (RDS, *O → *OOH), with the corresponding ΔG reduced from 2.08 eV to 1.58 eV.

OER overpotential (η) is commonly used as a core metric to quantify catalytic activity, and η exhibits a strong correlation with the adsorption energies of key intermediates (*OH, *O, *OOH) in the reaction pathway [78,79]. Addressing this critical scientific challenge, a study developed a convolutional neural network (CNN) model based on projected DOS features [80]. This model enables precise prediction of intermediate adsorption energies directly from the electronic structure characteristics of active sites. Three high-performance doped structures were selected through the ML framework: $Ru_{41}Zn_7O_{96}$, $Ru_{41}Fe_3Zn_4O_{96}$, and $Ru_{39}Co_1Cu_4Zn_4O_{96}$. These structures outperformed pure $RuO_{22}$ and previously reported catalysts in both stability ($\Delta E_{mix} < -0.05$ eV/atom) and activity ($\eta < 0.3$ V). This model overcomes limitations of traditional d-band theories, achieving mean absolute error values as low as 0.074 eV and 0.142 eV for OH and *O adsorption energies, significantly outperforming simple descriptor models.

While Ru-based catalysts have demonstrated remarkable performance at the laboratory scale, their large-scale application remains constrained. Future research should focus on atomically precise design (e.g., single-atom-cluster cascade catalysis), biomimetic structure construction (mimicking microenvironment regulation of enzyme active sites), and full-cell adaptation (optimizing interface contact with membrane electrode assemblies to reduce mass transfer resistance). Concurrently, integrating in-situ electron microscopy, synchrotron radiation, and AI is essential to establish a multiscale "structure-dynamics-performance" model. Through multidisciplinary collaboration, Ru-based catalysts hold promise to overcome the "activity-stability-cost" trade-off, positioning them as a core technology for acidic water electrolysis hydrogen production.

### 4.3. From lab to industry: catalysts for PEMWE

Multiple gaps remain before catalysts can truly transition from the

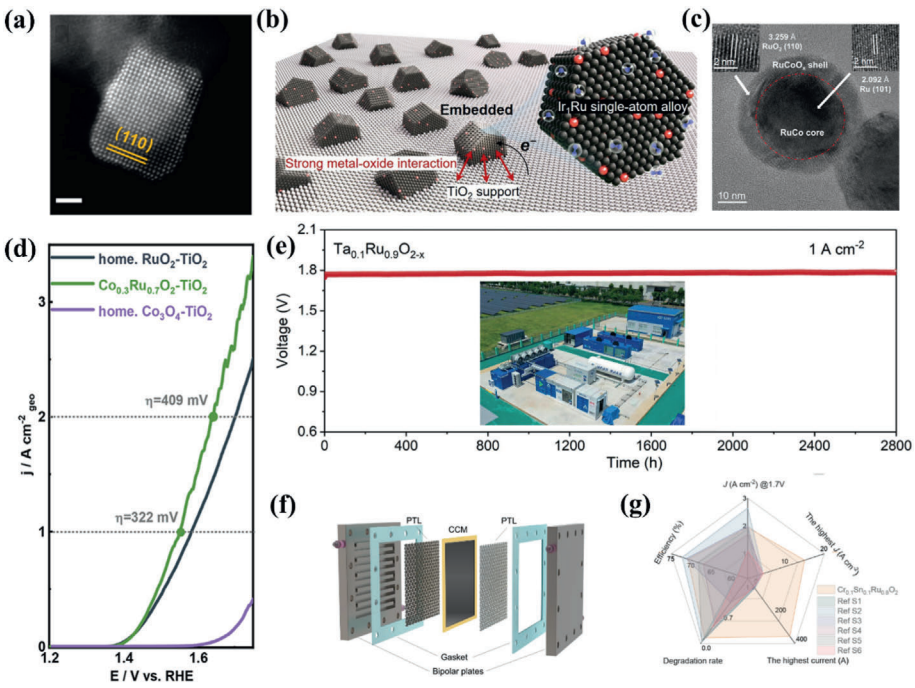


**Fig. 6.** (a) Atomic-scale HAADF-STEM characterization of Er-$RuO_X$ was conducted, scale bar: 2 nm [72]. Copyright 2024, Springer Nature. (b) Structural schematic of the $Ir_1Ru/TiO_2$ catalyst, with Ir atoms anchored on Ru NPs embedded within $TiO_2$ [51]. Copyright 2025, Wiley-VCH. (c) TEM image of Co-Ru@$RuO_2$ 9:1 nanoparticles with a core−shell heterostructure [10]. Copyright 2025, American Chemical Society. (d) Representative LSV curves for home. $RuO_2$−$TiO_2$, home. $Co_3O_4$−$TiO_2$, and $Co_{0.3}Ru_{0.7}O_2$−$TiO_2$ in 0.5 M $H_2SO_4$ at a scan rate of 10 mV $s^{-1}$ [74]. Copyright 2025, American Chemical Society. (e) Voltage-time curves of PEMWE with $Ta_{0.1}Ru_{0.9}O_{2-x}$ and a demonstration project in which solar-powered hydrogen production (of up to megawatt outputs) directly feeds a hydrogen refueling station [75]. Copyright 2025, AAAS. (f) Schematic of the PEMWE device [76]. Copyright 2025, American Chemical Society. (g) A radar diagram comparing PEMWE performance metrics of $Cr_{0.1}Sn_{0.1}Ru_{0.8}O_2$ with reference samples [77]. Copyright 2025, Wiley-VCH.

laboratory to stable industrialization [81–83]: Stability requirements: Industrial PEMWE systems must achieve >40,000 h of lifetime (approximately 5 years), whereas laboratory testing is often limited to 1000–3000 h [53,74,77]. Issues such as noble metal dissolution, support corrosion, and membrane degradation during long-term operation remain unresolved. Current Density and Efficiency: Industrial targets aim for >2 A $cm^{-2}$ current density at 1.8–1.9 V (U S. Department of Energy target) (Fig. 6d). While laboratory systems approach this threshold [84], bubble management and mass transfer limitations become more pronounced at high current densities in actual large-scale electrolyzers. Cost and Scalability: Noble metal loading must be further reduced to <0.1 mg $cm^{-2}$ (currently typically 0.2–0.5 mg $cm^{-2}$). Cr/Sn doping has lowered anode noble metal costs to 0.0069 USD $cm^{-2}$, but large-scale synthesis of catalyst coating membranes involves high process complexity and low yield. System Integration Challenges: Laboratory studies typically employ small-area electrodes (≤5 $cm^2$), whereas industrialization requires scaling to >1000 $cm^2$. Key bottlenecks during scaling include catalyst layer uniformity, interfacial contact resistance, and mechanical stability [74]. Therefore, collaborative research among industry, academia, and research institutions is essential to address these issues. Future research should integrate multidisciplinary tools to accelerate lifespan testing methods: developing accelerated degradation protocols that more closely mimic real-world operating conditions. Exploring low-cost supports: such as developing synergistic systems combining more stable $TiO_2$, carbon materials, and trace noble metals. Conducting engineering optimization: structural design targeting mass transfer and thermal management for large-scale electrolyzers. These efforts hold promise for accelerating the transition of catalysts from laboratory to industrial applications. Through a data-driven paradigm, noble metal catalyst R&D is advancing toward a new phase of "on-demand design," providing core material support for green energy technologies.

Laboratory studies have significantly enhanced the activity and stability of acidic OER catalysts in PEMWE devices through strategies such as atomic-level regulation, interfacial engineering, and strain engineering (Fig. 6f). Key advances include: Single-atom alloy design (Fig. 6b): Ir-Ru single-atom alloy ($Ir_1Ru/TiO_2$) stabilizes Ru sites via Ir atom pinning [51], achieving 144 mV overpotential at 10 mA $cm^{-2}$ in 0.5 M $H_2SO_4$ and stable operation for 2000 h (2 A $cm^{-2}$) in PEMWE. Multicomponent doping strategy [77]: $Cr_{0.1}Sn_{0.1}Ru_{0.8}O_2$ employs synergistic Cr and Sn doping to regulate interfacial proton consumption, achieving 3.0 A $cm^{-2}$ at 1.77 V with 1000-h stable operation (500 mA $cm^{-2}$) in PEMWE (Fig. 6g). $Co_{0.3}Ru_{0.7}O_2$-$TiO_2$ utilizes Co doping and a $TiO_2$ support layer to promote dual-site parallel oxidation pathways [74], achieving an overpotential of only 322 mV@1 A $cm^{-2}$. Nanostructure optimization: The porous Ir honeycomb structure electrode employs a templating method to fabricate a high-surface-area catalyst [53], achieving 1.842 V@2 A $cm^{-2}$ in PEMWE with a mass activity of 4.16 A $mg^{-1}$. Strain and Electronic Structure Modulation: Pt-$RuO_2$ exhibits Pt-induced strain heterogeneity [84], balancing lattice oxygen and adsorbate evolution mechanisms to achieve 3 A $cm^{-2}$@1.791 V in PEMWE. 4f-$RuO_2$ (e.g., Nd-$RuO_2$) modulates Ru-O polarity via rare earth elements [85], reducing overpotential to 214 mV.

Furthermore, a small number of noble metal catalysts have now entered the pilot-scale testing stage. For instance, Ta-$RuO_2$ catalysts demonstrated significant suppression of Ru dissolution in acidic OER tests [75], where Ta doping significantly suppressed Ru dissolution (Fig. 6e). At 1.6 V vs. RHE, the Ru dissolution rate decreased from 44.5 ng $h^{-1}$ for pure $RuO_2$ (on the (110) plane) to 21.8 ng $h^{-1}$, nearly doubling the stability parameter. Ta-$RuO_2$ exhibited $IrO_2$-like durability during long-term operation. Stability is a critical metric for industrial applications. Industrial demonstrations further validate Ta-$RuO_2$'s suitability. Within a large 625 $cm^2$ MEA, $Ta_{0.1}Ru_{0.9}O_{2-X}$ achieved a 625 A current (equivalent to 1 A $cm^{-2}$) at a low voltage of 1.704 V, yielding a hydrogen production rate of 0.523 $Nm^3\ h^{-1}$ at 1 kW power. This project has integrated a megawatt-scale solar-driven hydrogen production system to supply hydrogen to refueling stations, marking the transition of Ta-$RuO_2$ from laboratory research to industrial application.

Acidic water electrolysis, as a core technology for green hydrogen production, relies heavily on the innovative design of noble metal electrocatalysts. Recently, it has been increasingly recognized that while traditional experimental methodologies can yield high-performance catalysts, they are hindered by trial-and-error processes, vast parameter spaces (e.g., multi-component alloys), high costs, and prolonged development cycles. Consequently, integrating AI into the screening of noble metal catalysts presents a promising solution. Data-driven approaches significantly accelerate material screening and optimization, effectively mitigating the "curse of dimensionality." Collectively, these technologies lay a solid foundation for the industrialization of PEMWE [75,86].

## 5. Summary and outlook

Noble metal electrocatalysts are characterized by highly tunable electronic structures and superior intrinsic catalytic activity, stemming from their partially filled d-orbitals. Coupled with their exceptional corrosion resistance in harsh acidic media and high-potential environments, these materials hold immense promise for green hydrogen production via water electrolysis. Nevertheless, their widespread application faces significant practical hurdles. Iridium (Ir)-based catalysts, while offering high activity and robust stability, are constrained by high costs and low atom economy. Conversely, ruthenium (Ru)-based catalysts, despite exhibiting superior activity, fall short of the durability requirements necessary for long-term industrial operation.

This review presents a systematic review of noble metal-based electrocatalysts for acidic water splitting, encompassing Ir-, Ru-, and Pt-based materials and their derivatives. It comprehensively elucidates the fundamental mechanisms of the OER and HER in acidic media, alongside advanced catalyst design strategies. Despite significant advancements in acid-mediated electrocatalysis, practical barriers persist for large-scale PEMWE deployment: (1) Stability issues: Long-term durability is compromised by noble metal dissolution, support corrosion, and membrane degradation, falling short of industrial lifespan requirements; (2) Performance challenges: Gas bubble accumulation and mass transfer limitations severely hamper reaction efficiency at high current densities; (3) Cost and scalability bottlenecks: High noble metal loading drives up costs, while the fabrication of large-area catalyst-coated membranes (CCMs) remains complex with low yields; (4) System integration difficulties: Upscaling electrode areas exacerbates issues such as catalyst layer non-uniformity, interfacial contact resistance, and mechanical instability.

Furthermore, this review highlights the synergistic role of artificial intelligence (AI) in empowering the data-driven R&D of noble metal catalysts. This empowerment is primarily manifested in three key aspects: (1) Data mining and screening: Extracting critical insights from vast literature and databases to guide material pre-screening; (2) Automated experimentation: Efficiently executing repetitive synthesis and testing via robotic platforms to minimize human error and increase throughput; (3) Machine learning analysis: Utilizing algorithms to fit experimental data and deeply analyze the correlations between synthesis parameters and catalytic performance.

Finally, this review offers a forward-looking perspective. By further integrating interdisciplinary tools like AI, we can accelerate the transition of catalysts from laboratory research to industrial application, providing critical material support for achieving large-scale breakthroughs in green energy technologies.

## CRediT authorship contribution statement

**Xuan Yang:** Writing – review & editing, Writing – original draft, Investigation, Conceptualization. **Chenfei Xu:** Supervision, Formal analysis. **Ziqi Fu:** Formal analysis. **Xiaoyang Wang:** Supervision,

Formal analysis. **Yanan Chen:** Supervision, Funding acquisition, Conceptualization.

## Declaration of competing interest

The authors declare that they have no known competing financial interests or personal relationships that could have appeared to influence the work reported in this paper.

## Acknowledgements

We acknowledge financial supports from National Natural Science Foundation of China (Grant Nos. 52171219, 92372107).

## References

[1] X. Wang, W. Pi, Z. Li, S. Hu, H. Bao, W. Xu, N. Yao, Orbital-level band gap engineering of $RuO_2$ for enhanced acidic water oxidation, Nat. Commun. 16 (2025) 4845, https://doi.org/10.1038/s41467-025-60083-y.

[2] J. Li, H. Cheng, Y. Sun, R. Ma, D. Li, Y. Xu, J. Jin, X. Liu, M. Shao, L. Wang, Scalable ruthenium core–shell hydrogen catalyst for efficient and robust proton-exchange membrane electrolyser, Nat. Mater. (2025), https://doi.org/10.1038/s41563-025-02405-5.

[3] M. Huo, H. Sun, Z. Jin, W. Liu, Y. Liang, J. Liu, C. Liu, Z. Xing, Y. Yang, J. Chang, Tailoring octahedron-tetrahedron synergism in spinel catalysts for acidic water electrolysis, J. Am. Chem. Soc. 147 (2025) 10678–10689, https://doi.org/10.1021/jacs.5c00665.

[4] J. Tao, R. Gao, G. Lin, C. Chu, Y. Sun, C. Yu, Y. Ma, H. Qiu, Synthesis of noble metal nanoarrays via agglomeration and metallurgy for acidic water electrolysis, Nat. Commun. 16 (2025) 4996, https://doi.org/10.1038/s41467-025-60419-8.

[5] C. Liu, Z. Wei, M. Cao, R. Cao, Pt nanodendrites with a PtIr alloy surface structure exhibit excellent stability toward acidic hydrogen evolution reaction, Nano Res. 17 (2024) 4844–4849, https://doi.org/10.1007/s12274-024-6454-3.

[6] Q. Zeng, J. Tang, Y. Ji, Q. Jiang, C. Xia, Recent developments in single-atom engineering Ir/Ru-based catalysts for the oxygen evolution reaction in acidic media, Adv. Energy Mater. (2025) e04414, https://doi.org/10.1002/aenm.202504414.

[7] G. Li, A. Priyadarsini, Z. Xie, S. Kang, Y. Liu, X. Chen, S. Kattel, J.G. Chen, Achieving higher activity of acidic oxygen evolution reaction using an atomically thin layer of IrOx over $Co_3O_4$, J. Am. Chem. Soc. (2025), https://doi.org/10.1021/jacs.4c17915.

[8] C. Wang, X. Wu, H. Sun, Z. Xu, X. Wang, M. Li, Y. Wang, Y. Tang, J. Jiang, K. Sun, G. Fu, An asymmetric RE–O–Ru unit with bridged oxygen vacancies accelerates deprotonation during acidic water oxidation, Energy Environ. Sci. 18 (2025) 4276–4287, https://doi.org/10.1039/D5EE00281H.

[9] X. Wang, H. Jang, Z. Li, H. Li, G. Li, M.G. Kim, X. Ji, Q. Qin, X. Liu, Boosting the OER activity of amorphous $IrO_X$ in acidic medium by tuning its electron structure using lanthanum salt nanosheets, New J. Chem. 47 (2023) 2619–2625, https://doi.org/10.1039/d2nj05464g.

[10] J. Chen, Y. Ma, C. Cheng, T. Huang, R. Luo, J. Xu, X. Wang, T. Jiang, H. Liu, S. Liu, T. Huang, L. Zhang, W. Chen, Cobalt-doped Ru@$RuO_2$ core–shell heterostructure for efficient acidic water oxidation in low-Ru-loading proton exchange membrane water electrolyzers, J. Am. Chem. Soc. 147 (2025) 8720–8731, https://doi.org/10.1021/jacs.4c18238.

[11] D. Yuan, X. Dou, Q. Zhang, C. He, C. Wu, Y. Li, W. Li, L. Yu, L. Zhang, H.K. Liu, S. X. Dou, J. Liang, Y. Dou, Independent tuning of intermediate energetics for enhanced oxygen evolution via synergistic defects, Adv. Funct. Mater. 35 (2025) 2417098, https://doi.org/10.1002/adfm.202417098.

[12] W. Shi, T. Shen, C. Xing, K. Sun, Q. Yan, W. Niu, X. Yang, J. Li, C. Wei, R. Wang, S. Fu, Y. Yang, L. Xue, J. Chen, S. Cui, X. Hu, K. Xie, X. Xu, S. Duan, Y. Xu, B. Zhang, Ultrastable supported oxygen evolution electrocatalyst formed by ripening-induced embedding, Science 387 (2025) 791–796, https://doi.org/10.1126/science.adr3149.

[13] S. Zhang, X. Ma, Y. He, Y. Zhu, Z. Wang, Amorphous mixed Ir–Mn oxide catalysts for the oxygen evolution reaction in PEM water electrolysis for $H_2$ production, Int. J. Hydrogen Energy 48 (2023) 10532–10544, https://doi.org/10.1016/j.ijhydene.2022.11.316.

[14] S.-B. Han, Y.-H. Mo, Y.-S. Lee, S.-G. Lee, D.-H. Park, K.-W. Park, Mesoporous iridium oxide/Sb-doped $SnO_2$ nanostructured electrodes for polymer electrolyte membrane water electrolysis, Int. J. Hydrogen Energy 45 (2020) 1409–1416, https://doi.org/10.1016/j.ijhydene.2019.11.109.

[15] H. Wang, S. Zhu, J. Deng, W. Zhang, Y. Feng, J. Ma, Transition metal carbides in electrocatalytic oxygen evolution reaction, Chin. Chem. Lett. 32 (2021) 291–298, https://doi.org/10.1016/j.cclet.2020.02.018.

[16] H. Wang, C. Lin, L. Tan, J. Shen, X. Wu, X. Pan, Y. Zhao, H. Zhang, Y. Sun, B. Mei, H.-D. Um, Q. Xiao, W. Jiang, X. Li, W. Luo, Atomic ga triggers spatiotemporal coordination of oxygen radicals for efficient water oxidation on crystalline $RuO_2$, Nat. Commun. 16 (2025) 3976, https://doi.org/10.1038/s41467-025-58346-9.

[17] D. Wu, K. Kusada, S. Yoshioka, T. Yamamoto, T. Toriyama, S. Matsumura, Y. Chen, O. Seo, J. Kim, C. Song, S. Hiroi, O. Sakata, T. Ina, S. Kawaguchi, Y. Kubota, H. Kobayashi, H. Kitagawa, Efficient overall water splitting in acid with anisotropic metal nanosheets, Nat. Commun. 12 (2021) 1145, https://doi.org/10.1038/s41467-021-20956-4.

[18] Q. Dang, H. Lin, Z. Fan, L. Ma, Q. Shao, Y. Ji, F. Zheng, S. Geng, S.-Z. Yang, N. Kong, W. Zhu, Y. Li, F. Liao, X. Huang, M. Shao, Iridium metallene oxide for acidic oxygen evolution catalysis, Nat. Commun. 12 (2021) 6007, https://doi.org/10.1038/s41467-021-26336-2.

[19] M. Yang, H. Wu, Z. Shi, Y. Wang, J. Yang, J. Ni, P. Wang, Y. Cheng, Z. Wang, M. Xiao, C. Liu, W. Xing, Degradation mechanisms and stabilization strategies of ruthenium-based catalysts for OER in the proton exchange membrane water electrolyzer, Prog. Nat. Sci. Mater. Int. 34 (2024) 207–222, https://doi.org/10.1016/j.pnsc.2024.02.015.

[20] S. Zhou, L. Shi, Y. Li, T. Yang, S. Zhao, Metal-organic framework-based electrocatalysts for acidic water splitting, Adv. Funct. Mater. 34 (2024) 2400767, https://doi.org/10.1002/adfm.202400767.

[21] B. Deng, Z.-Y. Wu, E. Feng, L. Ma, Z. Wang, J. Chen, L. Eddy, A. Lathem, T. Wang, W. Chen, Y. Cheng, S. Xu, Q. Liu, B.I. Yakobson, H. Wang, Y. Zhao, J.M. Tour, Coupling amorphization and compositional optimization of ternary metal phosphides toward high-performance electrocatalytic hydrogen production, J. Am. Chem. Soc. 147 (2025) 16129–16140, https://doi.org/10.1021/jacs.5c00071.

[22] H. Zhang, Q. Zhang, X. Zeng, Construction of multiple heterogeneous interfaces and oxygen evolution reaction of hollow CoFe bimetallic phosphides derived from MOF template, Prog. Nat. Sci. Mater. Int. 34 (2024) 913–920, https://doi.org/10.1016/j.pnsc.2024.09.001.

[23] C. Rong, X. Shen, Y. Wang, L. Thomsen, T. Zhao, Y. Li, X. Lu, R. Amal, C. Zhao, Electronic structure engineering of single-atom Ru sites via Co–N4 sites for bifunctional pH-universal water splitting, Adv. Mater. 34 (2022) 2110103, https://doi.org/10.1002/adma.202110103.

[24] S. Zhang, Y. Chen, W. Hu, J. Hu, S. Cao, M. Du, Q. Li, Z. Lin, C. Pei, Y. Xu, M. Zheng, H. Pang, A versatile derivation approach to synthesize porous heterometallic phosphide and sulfide nanospheres for boosted oxygen evolution electrocatalysis, Prog. Nat. Sci. Mater. Int. 35 (2025) 1048–1054, https://doi.org/10.1016/j.pnsc.2025.09.008.

[25] Y. Chen, C. Shang, X. Xiao, W. Guo, Q. Xu, Recent progress of electrocatalysts for acidic oxygen evolution reaction, Coord. Chem. Rev. 508 (2024) 215758, https://doi.org/10.1016/j.ccr.2024.215758.

[26] J. Li, M. Guo, X. Yang, J. Wang, K. Wang, A. Wang, F. Lei, P. Hao, J. Xie, B. Tang, Dual elemental modulation in cationic and anionic sites of the multi-metal prussian blue analogue pre-catalysts for promoted oxygen evolution reaction, Prog. Nat. Sci. Mater. Int. 32 (2022) 705–714, https://doi.org/10.1016/j.pnsc.2022.12.001.

[27] L. Wang, Q. Meng, M. Xiao, C. Liu, W. Xing, J. Zhu, Insights into the dynamic surface reconstruction of electrocatalysts in oxygen evolution reaction, Renewables 2 (2024) 272–296, https://doi.org/10.31635/renewables.024.202400064.

[28] C. Lin, J.-L. Li, X. Li, S. Yang, W. Luo, Y. Zhang, S.-H. Kim, D.-H. Kim, S.S. Shinde, Y.-F. Li, Z.-P. Liu, Z. Jiang, J.-H. Lee, In-situ reconstructed Ru atom array on α-$MnO_2$ with enhanced performance for acidic water oxidation, Nat. Catal. 4 (2021) 1012–1023, https://doi.org/10.1038/s41929-021-00703-0.

[29] Y. Wang, Y. Qin, R. Wen, L. Wang, M. Dou, F. Wang, High-performance low-iridium catalyst for water oxidation: breaking long-ranged order of $IrO_2$ by neodymium doping, Small 20 (2024) 2401964, https://doi.org/10.1002/smll.202401964.

[30] R. Boppella, P.M. Austeria, G.H. Gu, T.K. Kim, Strongly coupled metal/amorphous $Ru/RuO_X$ heterostructure for efficient electrocatalytic hydrogen production, ACS Catal. 15 (2025) 16981–16991, https://doi.org/10.1021/acscatal.5c04859.

[31] Z. Li, H. Zhong, X. Liu, F. Chiang, R. Li, H. Chen, X. Wang, C. Wan, Y. Wu, H. Wang, S. Jiang, X. Zhang, Z. Lu, Dynamic dissolution-deposition equilibrium enables unprecedented HER stability in acidic PEMWE, Adv. Mater. (2025) e10703, https://doi.org/10.1002/adma.202510703.

[32] Q. Wang, W. Ling, Y. Lu, H. Zhao, Q. Cheng, Y. Huang, L. Zu, B. Yang, H. Yang, Synergistic stabilization of Pt single atoms by Cl and Ru for industrial-scale current density hydrogen production, Angew. Chem. Int. Ed. 64 (2025) e202506619, https://doi.org/10.1002/anie.202506619.

[33] Y. Yang, D. Pang, C. Wang, Z. Fu, N. Liu, J. Liu, H. Wu, B. Jia, Z. Guo, X. Fan, J. Zheng, Vacancy and dopant Co-constructed active microregion in Ru–$MoO_{3-x}$/$Mo_2AlB_2$ for enhanced acidic hydrogen evolution, Angew. Chem. Int. Ed. 64 (2025) e202504084, https://doi.org/10.1002/anie.202504084.

[34] R. Qin, G. Chen, X. Feng, J. Weng, Y. Han, Ru/Ir-based electrocatalysts for oxygen evolution reaction in acidic conditions: from mechanisms, optimizations to challenges, Adv. Sci. 11 (2024) 2309364, https://doi.org/10.1002/advs.202309364.

[35] Y. Qin, T. Yu, S. Deng, X.-Y. Zhou, D. Lin, Q. Zhang, Z. Jin, D. Zhang, Y.-B. He, H.-J. Qiu, L. He, F. Kang, K. Li, T.-Y. Zhang, $RuO_2$ electronic structure and lattice strain dual engineering for enhanced acidic oxygen evolution reaction performance, Nat. Commun. 13 (2022) 3784, https://doi.org/10.1038/s41467-022-31468-0.

[36] J. Zhang, L. Xu, X. Yang, S. Guo, Y. Zhang, Y. Zhao, G. Wu, G. Li, Amorphous $MnRuO_x$ containing microcrystalline for enhanced acidic oxygen-evolution activity and stability, Angew. Chem., Int. Ed. 63 (2024) e202405641, https://doi.org/10.1002/anie.202405641.

[37] H. Jun, E. Kang, J. Moon, H. Kim, S. Han, S. Choung, S. Kim, S.Y. Yi, E. Kang, C. H. Choi, J.W. Han, J. Lee, Quantity effect of heteroatom incorporation on the oxygen evolution mechanism in ruthenium oxide, Chem 11 (2025) 102367, https://doi.org/10.1016/j.chempr.2024.11.005.

[38] Y. Xu, Z. Mao, J. Zhang, J. Ji, Y. Zou, M. Dong, B. Fu, M. Hu, K. Zhang, Z. Chen, S. Chen, H. Yin, P. Liu, H. Zhao, Strain-modulated Ru-O covalency in Ru-Sn oxide enabling efficient and stable water oxidation in acidic solution, Angew. Chem. Int. Ed. 63 (2024) e202316029, https://doi.org/10.1002/anie.202316029.

[39] Y. Yang, J. Guo, L. Xu, C. Li, R. Ning, J. Ma, S. Geng, Bond engineering: weakening Ru–O covalency for efficient and stable water oxidation in acidic solutions, J. Energy Chem. 102 (2025) 1–9, https://doi.org/10.1016/j.jechem.2024.09.070.

[40] J.-Y. Chen, J.-T. Yang, Y.-S. Han, Y.-Q. Huang, N.-N. Tian, J.-H. Li, Z.-L. Wang, Passivation engineering toward integrated acidic oxygen evolution electrodes with stable catalytic activity for over 3000 h, ACS Catal. 15 (2025) 14882–14894, https://doi.org/10.1021/acscatal.5c02864.

[41] T. Wang, J. Hu, R. Ouyang, Y. Wang, Y. Huang, S. Hu, W.-X. Li, Nature of metal-support interaction for metal catalysts on oxide supports, Science 386 (2024) 915–920, https://doi.org/10.1126/science.adp6034.

[42] Z. Fu, P. Huang, X. Wang, W. Liu, L. Kong, K. Chen, J. Li, Y. Chen, Artificial intelligence-assisted ultrafast high-throughput screening of high-entropy hydrogen evolution reaction catalysts, Adv. Energy Mater. 15 (2025) 2500744, https://doi.org/10.1002/aenm.202500744.

[43] L. Zhou, M. Yang, Y. Liu, F. Kang, R. Lv, Intrinsic metal-support interactions break the activity-stability dilemma in electrocatalysis, Nat. Commun. 16 (2025) 8739, https://doi.org/10.1038/s41467-025-63397-z.

[44] P.B. Jørgensen, K.W. Jacobsen, M.N. Schmidt, Neural message passing with edge updates for predicting properties of molecules and materials. https://doi.org/10.48550/ARXIV.1806.03146, 2018.

[45] A.L. Maulana, S. Han, Y. Shan, P.-C. Chen, C. Lizandara-Pueyo, S. De, K. Schierle-Arndt, P. Yang, Stabilizing Ru in multicomponent alloy as acidic oxygen evolution catalysts with machine learning-enabled structural insights and screening, J. Am. Chem. Soc. 147 (2025), https://doi.org/10.1021/jacs.4c16638 jacs.4c16638.

[46] J. Abed, J. Heras-Domingo, R.Y. Sanspeur, M. Luo, W. Alnoush, D.M. Meira, H. Wang, J. Wang, J. Zhou, D. Zhou, K. Fatih, J.R. Kitchin, D. Higgins, Z.W. Ulissi, E.H. Sargent, Pourbaix machine learning framework identifies acidic water oxidation catalysts exhibiting suppressed ruthenium dissolution, J. Am. Chem. Soc. 146 (2024) 15740–15750, https://doi.org/10.1021/jacs.4c01353.

[47] Z. Zhang, Z. Ren, C.-W. Hsu, W. Chen, Z.-W. Hong, C.-F. Lee, A. Penn, H. Xu, D. J. Zheng, S. Miao, Y. Huang, Y. Gao, W. Chen, H. Smith, Y. Niu, Y. Tian, Y.-R. Lu, Y.-C. Shao, S. Li, H.-T. Wang, I.I. Abate, P. Agrawal, Y. Shao-Horn, J. Li, A multimodal robotic platform for multi-element electrocatalyst discovery, Nature 647 (2025) 390–396, https://doi.org/10.1038/s41586-025-09640-5.

[48] A.S. Nair, L. Foppa, M. Scheffler, Materials-discovery workflow guided by symbolic regression for identifying acid-stable oxides for electrocatalysis, npj Comput. Mater. 11 (2025) 150, https://doi.org/10.1038/s41524-025-01596-4.

[49] L. Xu, L. Lu, N. Xu, J. Huang, G. Li, J. Wang, X. Hu, A. Guerrero, J.C.V. Reyes, X. Xu, Z. Han, Z. Chen, Progressive learning-guided discovery of single-atom metal oxide catalysts for acidic oxygen evolution reaction, Angew. Chem. Int. Ed. 64 (2025) e202510965, https://doi.org/10.1002/anie.202510965.

[50] L. Zhang, Q. Bing, H. Qin, L. Yu, H. Li, D. Deng, Artificial intelligence for catalyst design and synthesis, Matter 8 (2025) 102138, https://doi.org/10.1016/j.matt.2025.102138.

[51] S. Li, L. Deng, S. Hung, S. Zhao, L. Wang, Y. Hao, Y. Long, B. Li, Y. Hsu, Y. Chen, Y. Zhang, T. Chen, F. Hu, L. Li, Y. Hu, Y. Wu, S. Peng, Embedded Ir—Ru single-atom alloy with self-limiting motifs for sustainable proton exchange membrane water electrolysis, Adv. Mater. (2025) e07340, https://doi.org/10.1002/adma.202507340.

[52] Y.H. Yun, K. Yoon, S. Byun, H. Park, G. Doo, S. Kim, M. Kim, H.-S. Cho, B.-S. An, B. Koo, C. Lee, Hollow $Bi_2Te_3$ nanowire supported ir for highly active and durable oxygen evolution reaction in proton exchange membrane water electrolysis, Nano Res. 18 (2025) 94908097, https://doi.org/10.26599/NR.2025.94908097.

[53] L. Ding, W. Wang, Z. Xie, K. Li, S. Yu, C.B. Capuano, A. Keane, K. Ayers, F.-Y. Zhang, Highly porous iridium thin electrodes with low loading and improved reaction kinetics for hydrogen generation in PEM electrolyzer cells, ACS Appl. Mater. Interfaces 15 (2023) 24284–24295, https://doi.org/10.1021/acsami.2c23304.

[54] J. Li, C. Tang, Y. Zhou, R. Hong, M. Fang, L. Xing, N. Wang, L. Meng, S. Ye, L. Du, Progress of Ir/Ru-based catalysts for electrocatalytic oxygen evolution reaction in acidic environments, Int. J. Hydrogen Energy 92 (2024) 657–671, https://doi.org/10.1016/j.ijhydene.2024.10.277.

[55] A. Kumar, M. Gil-Sepulcre, J.P. Fandré, O. Rüdiger, M.G. Kim, S. DeBeer, H. Tüysüz, Regulating local coordination sphere of Ir single atoms at the atomic interface for efficient oxygen evolution reaction, J. Am. Chem. Soc. 146 (2024) 32953–32964, https://doi.org/10.1021/jacs.4c08847.

[56] L.E. Camacho-Forero, F. Godínez-Salomón, G. Ramos-Sánchez, C.P. Rhodes, P. B. Balbuena, Theoretical and experimental study of the effects of cobalt and nickel doping within $IrO_2$ on the acidic oxygen evolution reaction, J. Catal. 408 (2022) 64–80, https://doi.org/10.1016/j.jcat.2022.02.016.

[57] L. Wang, J. Zhou, Y. Zhou, K. Liu, L. Ke, H. Li, S. Liu, X. Wang, W. Zhu, Y. Li, K. Yao, S. Huang, Y. Liu, H. Liang, Oxygen vacancy-mediated oxide pathway mechanism in proton-exchange membrane water electrolysis, Adv. Funct. Mater. (2025) e16646, https://doi.org/10.1002/adfm.202516646.

[58] Z. Liu, G. Wang, J. Guo, S. Wang, S. Zang, Sub-2 nm $IrO_2$/Ir nanoclusters with compressive strain and metal vacancies boost water oxidation in acid, Nano Res. 16 (2023) 334–342, https://doi.org/10.1007/s12274-022-4807-3.

[59] J. Zhao, Y. Guo, Z. Zhang, X. Zhang, Q. Ji, H. Zhang, Z. Song, D. Liu, J. Zeng, C. Chuang, E. Zhang, Y. Wang, G. Hu, M.A. Mushtaq, W. Raza, X. Cai, F. Ciucci, Out-of-plane coordination of iridium single atoms with organic molecules and cobalt–iron hydroxides to boost oxygen evolution reaction, Nat. Nanotechnol. 20 (2025) 57–66, https://doi.org/10.1038/s41565-024-01807-x.

[60] H. Zhu, Y. Wang, Z. Jiang, B. Deng, Y. Xin, Z. Jiang, Defect engineering promoted ultrafine Ir nanoparticle growth and Sr single-atom adsorption on $TiO_2$ nanowires to achieve high-performance overall water splitting in acidic media, Adv. Energy Mater. 14 (2024) 2303987, https://doi.org/10.1002/aenm.202303987.

[61] Q. Li, Y. Feng, Y. Yu, Y. Chen, Y. Xie, F. Luo, Z. Yang, Engineering $e_g$ filling of $RuO_2$ enables a robust and stable acidic water oxidation, Chin. Chem. Lett. 36 (2025) 110612, https://doi.org/10.1016/j.cclet.2024.110612.

[62] M. Sun, H. Huang, X. Niu, S. Gong, Z. Li, J. Fang, X. Liu, Y. Chen, H. Duan, Z. Zhuang, S. Nagao, Y. Aoki, L. Zhang, Z. Niu, Grain boundary-derived local amorphization enhances acidic OER, ACS Catal. 14 (2024) 15764–15776, https://doi.org/10.1021/acscatal.4c03746.

[63] H.N. Nong, T. Reier, H.-S. Oh, M. Gliech, P. Paciok, T.H.T. Vu, D. Teschner, M. Heggen, V. Petkov, R. Schlögl, T. Jones, P. Strasser, A unique oxygen ligand environment facilitates water oxidation in hole-doped $IrNiO_X$ core–shell electrocatalysts, Nat. Catal. 1 (2018) 841–851, https://doi.org/10.1038/s41929-018-0153-y.

[64] M. Kost, M. Kornherr, P. Zehetmaier, H. Illner, D.S. Jeon, H. Gasteiger, M. Döblinger, D. Fattakhova-Rohlfing, T. Bein, Chemical epitaxy of iridium oxide on tin oxide enhances stability of supported OER catalyst, Small 20 (2024) 2404118, https://doi.org/10.1002/smll.202404118.

[65] X. Niu, Y. Chen, M. Sun, S. Nagao, Y. Aoki, Z. Niu, L. Zhang, Bayesian learning-assisted catalyst discovery for efficient iridium utilization in electrochemical water splitting, Sci. Adv. 11 (2025), https://doi.org/10.1126/sciadv.adw0894 eadw0894.

[66] X. Lin, X. Du, S. Wu, S. Zhen, W. Liu, C. Pei, P. Zhang, Z.-J. Zhao, J. Gong, Machine learning-assisted dual-atom sites design with interpretable descriptors unifying electrocatalytic reactions, Nat. Commun. 15 (2024) 8169, https://doi.org/10.1038/s41467-024-52519-8.

[67] X. Zhu, W. Huang, Y. Lou, Z. Yao, H. Ying, M. Dong, L. Tan, J. Zeng, H. Ji, H. Zhu, S. Lan, Ultrafast joule-heating synthesis of FeCoMnCuAl high-entropy-alloy nanoparticles as efficient OER electrocatalysts, Prog. Nat. Sci. Mater. Int. 34 (2024) 880–887, https://doi.org/10.1016/j.pnsc.2024.08.005.

[68] X. Zhu, W. Huang, L. Tan, Z. Yao, X. Yang, R. Song, M. Chen, D. Liu, J. Zeng, H. Zhu, S. Lan, Ultrafast synthesis of tetragonal-distorted FeCoNiCuCr high-entropy alloy nanoparticles for enhanced OER performance, Chin. Chem. Lett. (2025) 110852, https://doi.org/10.1016/j.cclet.2025.110852.

[69] C. Cai, T. Wang, Resolving chemical-motif similarity with enhanced atomic structure representations for accurately predicting descriptors at metallic interfaces, Nat. Commun. 16 (2025) 8761, https://doi.org/10.1038/s41467-025-63860-x.

[70] C. Wang, L. Jin, H. Shang, H. Xu, Y. Shiraishi, Y. Du, Advances in engineering $RuO_2$ electrocatalysts towards oxygen evolution reaction, Chin. Chem. Lett. 32 (2021) 2108–2116, https://doi.org/10.1016/j.cclet.2020.11.051.

[71] Q. Wu, R. Zhou, Z. Yao, T. Wang, Q. Li, Effective approaches for enhancing the stability of ruthenium-based electrocatalysts towards acidic oxygen evolution reaction, Chin. Chem. Lett. 35 (2024) 109416, https://doi.org/10.1016/j.cclet.2023.109416.

[72] L. Li, G. Zhang, C. Zhou, F. Lv, Y. Tan, Y. Han, H. Luo, D. Wang, Y. Liu, C. Shang, L. Zeng, Q. Huang, R. Zeng, N. Ye, M. Luo, S. Guo, Lanthanide-regulating Ru-O covalency optimizes acidic oxygen evolution electrocatalysis, Nat. Commun. 15 (2024) 4974, https://doi.org/10.1038/s41467-024-49281-2.

[73] Y. Zhou, Y. Mao, C. Ye, Z. Wang, S. Wei, J.V. Kennedy, Y. Zhao, H. Yang, B.C. C. Cowie, G.I.N. Waterhouse, Ru single atoms anchored on $Co_3O_4$ nanorods for efficient overall water splitting under pH-universal conditions, Adv. Energy Mater. 15 (2025) 2500700, https://doi.org/10.1002/aenm.202500700.

[74] J. Liang, Y. Zhao, C. Yang, S. Zhu, L. Wang, K. Xu, X. Mu, Y. Han, Z. Liu, Z. Zhao, W. Liu, F. Li, Z. Peng, E.C.M. Tse, Q. Liu, J. Gao, Q. Li, J. Li, J. Liu, Dual-site cobalt-doped $RuO_2$ /$TiO_2$ electrocatalyst enables stable and cost-efficient acidic oxygen evolution for PEM water electrolysis, J. Am. Chem. Soc. 147 (2025) 39781–39795, https://doi.org/10.1021/jacs.5c14137.

[75] J. Zhang, X. Fu, S. Kwon, K. Chen, X. Liu, J. Yang, H. Sun, Y. Wang, T. Uchiyama, Y. Uchimoto, S. Li, Y. Li, X. Fan, G. Chen, F. Xia, J. Wu, Y. Li, Q. Yue, L. Qiao, D. Su, H. Zhou, W.A.G. Iii, Y. Kang, Tantalum-stabilized ruthenium oxide electrocatalysts for industrial water electrolysis, Science 387 (2025) 48–55, https://doi.org/10.1126/science.ado9938.

[76] M. Qi, X. Du, X. Shi, S. Wang, B. Lu, J. Chen, S. Mao, H. Zhang, Y. Wang, Single-atom Ru-Triggered lattice oxygen redox mechanism for enhanced acidic water oxidation, J. Am. Chem. Soc. 147 (2025) 18295–18306, https://doi.org/10.1021/jacs.5c05752.

[77] J. Bao, Y. Gu, B. Su, X. Sun, H. Zhang, K. Wang, X. Lin, C. Yang, B. Yang, Z. Li, C. Dong, Q. Zheng, M. Qiu, L. Lei, C. Yuan, Z. Shao, Y. Hou, Electronic structure-engineered proton depletion interfaces on ternary $RuO_2$ for ultra-stable kilowatt electrocatalysis, Angew. Chem. Int. Ed. 64 (2025) e202515362, https://doi.org/10.1002/anie.202515362.

[78] S. Yang, Y. Wang, Y. Gong, Anchoring ruthenium single atoms into the carbon nanotubes-supported nickel-based sulfides for enhanced electrocatalytic oxygen evolution, J. Colloid Interface Sci. 699 (2025) 138255, https://doi.org/10.1016/j.jcis.2025.138255.

[79] J. Tao, B. Fang, Z. Fang, G. Lin, Z. Ji, C. Gao, R. Gao, H. Qiu, Micellar brush-directed oxophilic Zr-doped $RuO_2$ nanoarrays for durable acidic oxygen evolution reaction, Angew. Chem. Int. Ed. 64 (2025) e202512348, https://doi.org/10.1002/anie.202512348.

[80] Z. Shang, S. Zhao, Q. Dang, F. Wang, X. Sun, H. Li, A general machine-learning framework for high-throughput screening for stable and efficient $RuO_2$ -based acidic oxygen evolution reaction catalysts, ACS Catal. 15 (2025) 12835–12847, https://doi.org/10.1021/acscatal.5c02247.

[81] M. Zhang, W. An, Q. Liu, Y. Jiang, X. Zhao, H. Chen, Y. Zou, X. Liang, X. Zou, Tunnel-structured $IrO_X$ unlocks catalytic efficiency in proton exchange membrane water electrolyzers, Nat. Commun. 16 (2025) 7608, https://doi.org/10.1038/s41467-025-62861-0.

[82] M.-R. Qu, H. Liu, S.-H. Feng, X.-Z. Su, J. Xu, H.-L. Duan, R.-Q. Liu, Y.-Y. Qin, W.-S. Yan, S. Zhu, R. Wu, H. Li, S.-H. Yu, Temperature-dependent mechanism evolution on $RhRu_3O_X$ for acidic water oxidation, Nat. Commun. 16 (2025) 9261, https://doi.org/10.1038/s41467-025-64286-1.

[83] C. Qiu, C. Sellers, Z.-Y. Wu, D.A. Cullen, E. Stavitski, A. Tayal, T.-U. Wi, M. Kodali, B. Erb, A. Smeltz, F.-Y. Chen, Y. Feng, Z. Yu, A. Elgazzar, T. Terlier, T.P. Senftle, H. Wang, Low-iridium stabilized ruthenium oxide anode catalyst for durable proton-exchange membrane water electrolysis, Nat. Nanotechnol. (2025), https://doi.org/10.1038/s41565-025-02030-y.

[84] X. Cao, L. Miao, W. Jia, H. Qin, G. Lin, R. Ma, T. Jin, L. Jiao, Strain heterogeneity in $RuO_2$ for efficient acidic oxygen evolution reaction in proton exchange membrane water electrolysis, Nat. Commun. 16 (2025) 6217, https://doi.org/10.1038/s41467-025-58570-3.

[85] X. Zhang, Y. Zhang, B.O. Protsenko, M.A. Soldatov, J. Zhang, C. Yang, S. Bo, H. Wang, X. Chen, C. Wang, W. Cheng, Q. Liu, 4*f*-modified Ru-O polarity as a descriptor for efficient electrocatalytic acidic oxygen evolution, Nat. Commun. 16 (2025) 6921, https://doi.org/10.1038/s41467-025-62258-z.

[86] H. Wu, Z. Fu, J. Chang, Z. Hu, J. Li, S. Wang, J. Yu, X. Yong, G.I.N. Waterhouse, Z. Tang, J. Chang, S. Lu, Engineering high-density microcrystalline boundary with V-doped $RuO_2$ for high-performance oxygen evolution in acid, Nat. Commun. 16 (2025) 4482, https://doi.org/10.1038/s41467-025-59472-0.